ISSN 0023-1584, Kinetics and Catalysis, 2014, Vol. 55, No. 3, pp. 278–286. © Pleiades Publishing, Ltd., 2014.

Benzene Combustion: A Detailed Chemical Kinetic Modeling in Laminar Flames Conditions[1]

Y. Rezgui* and M. Guemini

Laboratoire de Chimie Appliquée et Technologie des Matériaux, Université d'Oum El Bouaghi, Algérie

**e-mail: yacinereference@yahoo.com*

Received June 22, 2013

Abstract—Models resulting from the merging of validated kinetic schemes were used to compile a new detailed mechanism for benzene combustion in laminar flames. The proposed model, featuring 215 species and 1313 reactions, has been validated using fuel-rich, low-pressure, premixed benzene–oxygen–argon flames available in the literature. Good agreement between simulated and experimental data is achieved for the major reactants, intermediates, and products. However, computed maxima for some polyaromatic hydrocarbons were lower than experimental ones.

DOI: 10.1134/S0023158414030124

Due to its high density and antiknock rating, the combustion and the oxidation chemistries of the simplest aromatic hydrocarbon (benzene) have been the subject of numerous studies over the past few decades [1–8]. However, because of its carcinogenic effects, benzene usage was limited to a maximum of 1% by recent legislative action in the United States [1]. Despite its limited presence in fuels, benzene is ubiquitously formed during the combustion of hydrocarbons from methane used in spark-ignition engines, Diesel engines and aircrafts. In addition, aromatic compounds, especially benzene, are closely linked to the formation of polycyclic aromatic hydrocarbons (**PAH**) in the practical combustion systems. Besides being carcinogenic or mutagenic in them, PAH are intermediates in the formation of soot [9], chlorinated dioxins and furans [10]. As mentioned by Brukh et al. [11], under fuel rich conditions, the PAH compounds are likely to be formed by sequential activation of neighboring aromatic sites by hydrogen atom abstraction, followed by addition of the aryl radical to acetylene molecule. The repetition of the sequence H abstraction followed by acetylene addition leads to the cyclization to the next higher order ring (HACA mechanism). Therefore, a good understanding of the oxidation mechanism of the first aromatic ring (benzene), which is thought to be the main precursor of PAHs, is considered as one of the most interesting research subjects in the combustion society, from a fundamental and a practical point of view [12].

The combustion chemistry of benzene has been performed by many groups [6, 13–18], starting with the pioneering work of Bittner and Howard [6] who used molecular beam mass spectrometry (**MBMS**) as a mean to establish the structure of a benzene–oxygen–argon system burning at low pressure (26.7 mbar) and fuel rich conditions (equivalence ratio $\varphi = 1.8$). Using radical scavenging techniques, Richter et al. [13] have brought some supplementary data to the same flame. Meanwhile, Defoeux et al. have studied the structure of a rich ($\varphi = 2.0$) low-pressure ($P =$ 50 mbar) C_6H_6–O_2–Ar flame with the same method recently [4]. A comprehensive experimental study of a similar ($\varphi = 1.78$, $P = 4$ kPa) flame has been performed by Yang et al. [19] using tunable synchrotron photo ionization and MBMS. In this study, isomers of most observed species in the flame have been unambiguously identified by measurements of the photo ionization efficiency spectra. Mole fraction profiles of species up to $C_{16}H_{10}$ have been measured at the selective photon energies near ionization thresholds. Recently, Detilleux and Vandooren [5] reported gas chromatography data from one-dimensional laminar premixed benzene–oxygen–argon flames with equivalence ratios of 2, 1, and 0.7, stabilized at low pressure (45 mbar) on a flat flame burner.

To model these experimental data, detailed kinetic models have been proposed by Lindstedt and Skevis [20], Zhang and McKinnon [21], Tan and Frank [12], Ristori et al. [22], D'Anna and Violi [23] and Howard's group [3, 24]. These published models give qualitative agreement with many experimental measurements; however, agreement for some intermediate species is poor. In general, comparisons of these kinetic schemes confirm that important reaction paths are missing in these mechanisms and that further improvements were necessary for predicting intermediate species, such as diacetylene, cyclopentadienyl radical, cyclopentadiene, and vinylacetylene.

[1] The article is published in the original.

Recently, a detailed kinetic modeling study of benzene oxidation and combustion in premixed flames and ideal reactors was conducted by Vourliotakis et al. [25] and a comprehensive mechanism was proposed. The developed kinetic scheme captured well most of the species involved in the benzene combustion, however it is limited to C_6 species only and don't deal with heavier compounds. The most recent modeling work on benzene pyrolysis and oxidation was performed by Saggese et al. [26]. In this study, the proposed model, consisting of over 10000 reactions and more than 350 species, was developed based on hierarchically modularity and was validated against a huge set of experiments.

In this work, a new model for benzene combustion in laminar flames, based on the mechanism of Vourliotakis et al. [25] and extended to simulate C_{10} species, was developed. The developed kinetic mechanism was used to simulate the fuel-rich ($\varphi = 1.8$), low-pressure, premixed benzene-oxygen flame of Bittner and Howard [6] which is well-characterized, in terms of gaseous products and high molecular aromatics.

MODEL DEVELOPMENT PROCEDURE

The mechanism used in this work is based on the detailed kinetic model developed by Vourliotakis et al. [25] which was assessed against experimental data issued from studies which have been conducted in flames [4–6, 19], shock tubes [27], perfectly stirred and plug-flow reactors [7, 22, 28–30], all under a wide range of temperatures, pressures, and stoichiometries. Predictive capabilities of the model were found to be at least fair and often good to excellent for the consumption of the reactants, the formation of the main combustion products, and the formation and depletion of major intermediates including radicals. The mechanism was subsequently extended to PAH up to naphthalene ($C_{10}H_8$) and biphenyl ($C_{12}H_{10}$) [3, 31]. It is noteworthy that the kinetic submechanism for the formation of larger aromatic structures includes the replicating hydrogen abstraction carbon addition (**HACA**) mechanism as well as kinetic pathways involving resonantly stabilized free radicals.

We have also used, in our proposed model, some of the elementary reactions for HCO, C_2H_5, and CH_3O from the work of Hampson [32], those for methylene triplet from the work of Bohland et al. [33], and CH from the work of Bergeat et al. [34]. Besides, some CH_2CO and 1,2-butadiene elementary reactions, taken from the work of Hidaka et al. [35, 36] and Dagaut and Kurylo [37], have been added to the kinetic scheme. In addition, recent results, concerning methanol, obtained by our group have been incorporated in this model [38].

In order to have good prediction of propargyl radical (C_3H_3) profiles, oxidation reactions of propynylidene (1-C_3H_2) were added from the works [12] (in all next reactions the pre-exponential factor A is expressed in $cm^3\ mol^{-1}\ K^{-1}$, and activation energy is expressed in J)

1-$C_3H_2 + O_2 = HCCO + CO + H$
($k = 1.00 \times 10^{14}\exp(-12540.0/RT)$),
1-$C_3H_2 + OH = C_2H_2 + HCO$ ($k = 5.00 \times 10^{13}$),
$C_3H_3 + O =$ 1-$C_3H_2 + OH$ ($k = 3.00 \times 10^{12}$),

and [3]

1-$C_3H_2 + O = C_2H + HCO$ ($k = 6.80 \times 10^{13}$),
1-$C_3H_2 + O = C_2H_2 + CO$ ($k = 1.00 \times 10^{14}$).

Also some reactions of C_3H_3 were added from [39]

$C_2H + CH_2OH = C_3H_3 + OH$ ($k = 1.21 \times 10^{13}$),
$C_2H + C_2H_5 = CH_3 + C_3H_3$ ($k = 1.81 \times 10^{13}$),

and [3]

$C_3H_3 + O = C_2H_2 + CO + H$ ($k = 1.40 \times 10^{14}$),
$C_3H_3 + OH =$ l-$C_3H_2 + H_2O$ ($k = 1.00 \times 10^{13}$),
$C_3H_3 + C_3H_3 = C_6H_5 + H$ ($k = 1.00 \times 10^{13}$).

The proposed mechanism consists of 215 species evolved in 1313 reversible reactions and it distinguishes between singlet and triplet methylene as well as between structural isomers of C_4 species which are important in ring growth and rupture processes. More specifically, the model distinguishes between 1,3-butadiene ($CH_2CHCHCH_2$), 1,2-butadiene (CH_3CHCCH_2), 1-C_4H_6, 2-C_4H_6 and cyclo-C_4H_6 and the corresponding *n*–butadienyl ($CH_2CHCHCH$ and CH_3CHCCH) and *i*-butadienyl isomers (CH_2CHCCH_2). For C_4H_3, *n*-C_4H_3 (CHCCHCH) and *i*-C_4H_3 ($CHCCCH_2$) have been considered. In addition, fifteen linear species 1-C_3H_2, 1-C_5H_2, 1-C_5H_3, 1-C_5H_4, 1-C_5H_5, 1-C_5H_6, 1-C_5H_7, 1-C_6H_4, 1,3-C_6H_5, 1,5-C_6H_5, 1,2-C_6H_6, 1,3-C_6H_6, 1,5-C_6H_6, 1,2,4,5-C_6H_6 and 1-C_6H_7 were taken into account. The proposed mechanism, in Chemkin format, could be found by contacting the authors.

MODEL TESTING

All model calculations were performed with PREMIX flame code, a part of the CHEMKIN software package [40]. As mentioned by D'Anna and Violi [41], the PREMIX code computes the species profiles for a burner-stabilized premixed laminar flame, using the cold mass flow rate through the burner, feed-gas composition, pressure, and an estimated solution profile as input. The program can also compute the temperature profile. However, heat losses to the burner surface and the external environment are unknown; therefore, an experimentally determined temperature profile is used as input.

The reaction mechanism was tested against the MBMS data of Bittner and Howard [6] in a near sooting laminar premixed benzene–oxygen–argon flame (equivalence ratio $\varphi = 1.8$). The flame was stabilized on a cooled copper plate burner at 20 Torr. The initial

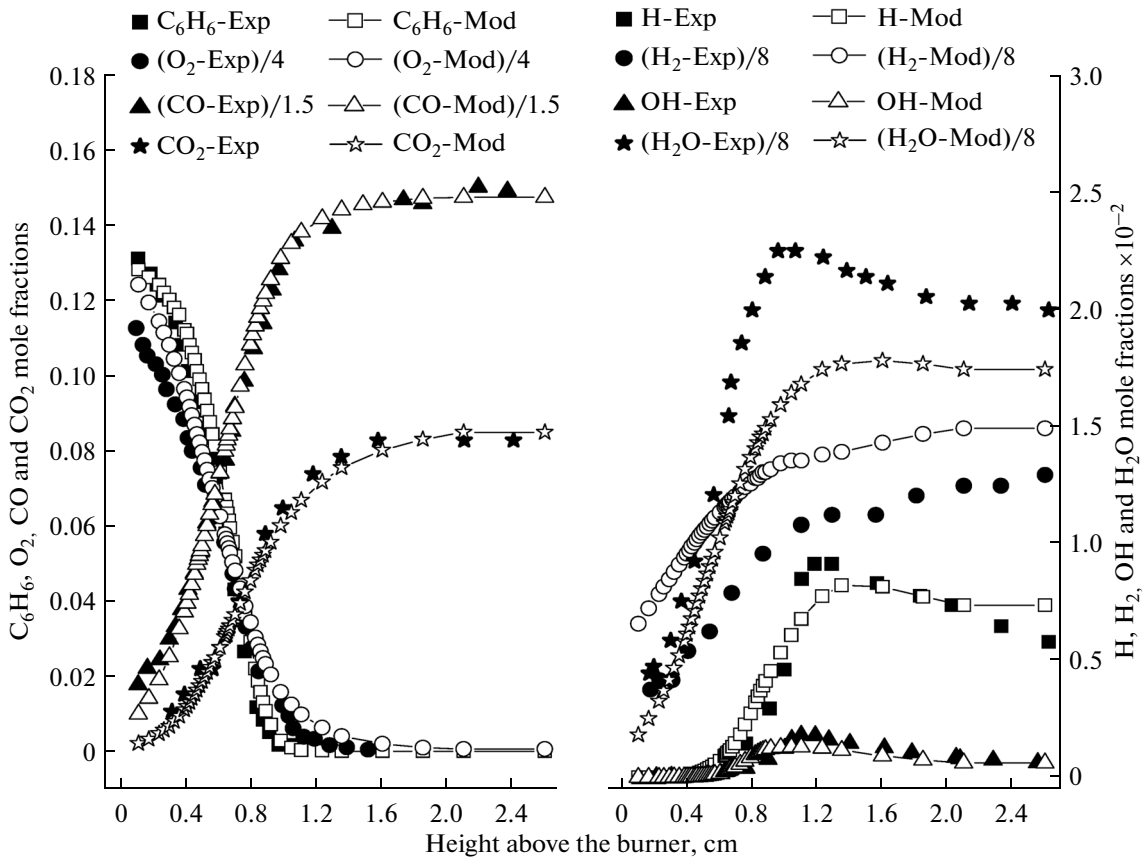

Fig. 1. Comparison between computed (lines + light symbols) and experimental ([6], dark symbols) C_6H_6, O_2, CO, CO_2, H, H_2, OH and H_2O mole fraction profiles.

reactant concentrations were 13.5 mol % benzene, 56.5 mol % oxygen, and 30 mol % argon at a cold gas velocity of 50 cm/s (298 K). It is noteworthy that, in our calculations, experimental mass flow rate through the burner, gas composition, pressure, temperature, and estimated initial solution profile were used as inputs.

RESULTS AND DISCUSSION

Model Validation

Simulated and experimental mole fraction profiles for C_6H_6, O_2, CO, CO_2, H, H_2, OH and H_2O are depicted in Fig. 1. Reactants (C_6H_6 and O_2) are extremely well reproduced by the current model. Benzene and oxygen concentrations rapidly decrease in the flame zone which is located at about 0.5 cm above the burner. Besides, except for H_2O where the model underpredicts the mole fraction by a factor of 1.3, all the other products (CO and CO_2) modelled concentration profiles are in good agreement with those measured experimentally.

Compared to concentrations of stable species, the concentrations of radicals are more difficult to measure and are known with larger uncertainty [3]. A very satisfactory prediction was observed for H and OH mole fraction profiles, whereas the H_2 concentration was somewhat overpredicted by the model (by a factor of 1.2). This over prediction was also reported by Vourliotakis et al. [25] during their modeling study on benzene oxidation and combustion in premixed flames and ideal reactors.

Computed and experimental mole fraction profiles of CH_3, CH_4, C_2H_2, C_3H_2, C_3H_3 and C_3H_4 are given in Fig. 2. The methyl radical and methane concentration profiles shapes were very well reproduced by the model, whereas their maximum peaks were overpredicted by a factor of 1.9 and 1.4, respectively. On the other hand, both shape and value of acetylene mole fraction were very well predicted by the proposed model. It is noteworthy could be said that, by comparison of our calculations with the ones given by the published models in the literature [5, 12, 41], our proposed model was able to predict, with a good level of accuracy, mole fraction profiles of C_1 and C_2 species.

Concerning the C_3 species, it can be seen that C_3H_3 and C_3H_4 mole fraction profiles were very well reproduced, whereas C_3H_2 was somewhat underpredicted (1.6 times) and shifted toward unburned gases. As

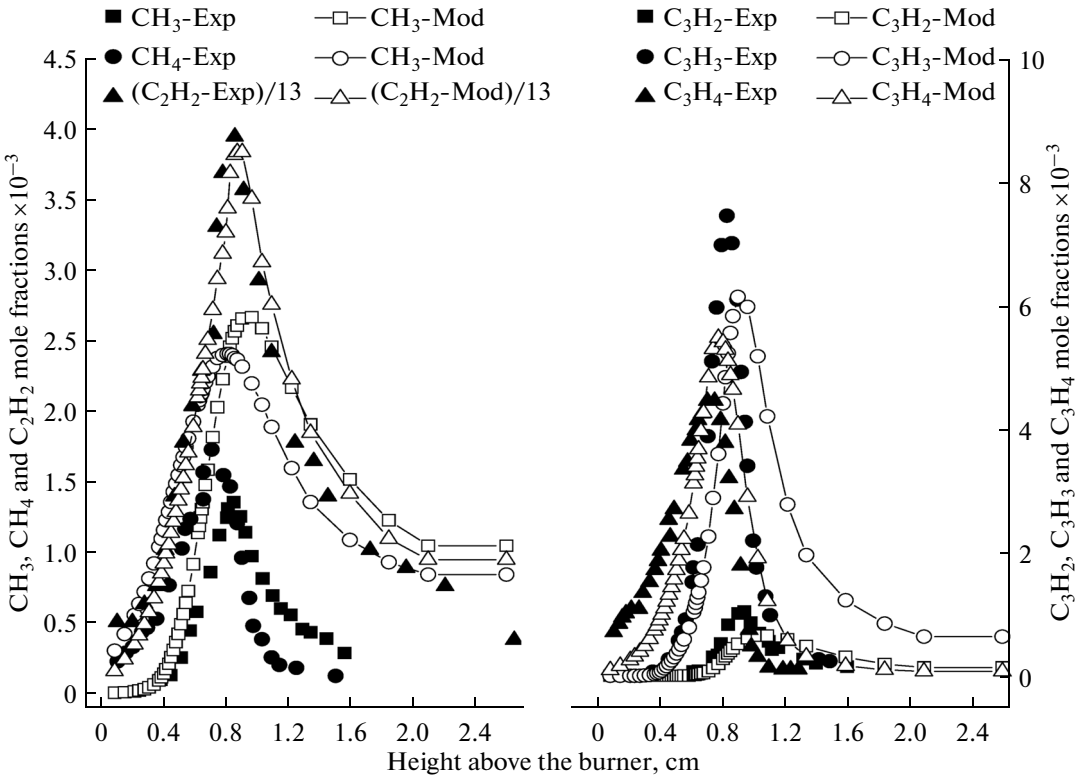

Fig. 2. Comparison between computed (lines + light symbols) and experimental ([6], dark symbols) CH_3, CH_4, C_2H_2, C_2H_2, C_3H_2, C_3H_3 and C_3H_4 mole fraction profiles.

compared to the model used by Lindstedt and Skevis [20] which underestimates the C_3H_2 maximum peak by a factor of 1.6 and to the models used by Djurisic et al. [42], Defoeux et al. [4], Vourliotakis et al. [25] and Ristori et al. [22] which overpredict the C_3H_2 maximum peak by a factor of 1.9, 10, 1.5 and 7, respectively, it could be said that our proposed model exhibits a very good capability in the prediction of the C_3 mole fraction profiles.

Mole predictions for C_5H_3, C_5H_5, C_5H_6, C_6H_5, C_7H_8, C_8H_2, C_8H_8, C_9H_8, $C_{10}H_8$, $C_{12}H_8$ and $C_{12}H_{10}$ are shown in Fig. 3. For C_5 species, it could be seen that our proposed model underpredicts the C_5H_3 maximum peak by a factor of 2, overpredicts the value of C_5H_6 by a factor of 1.2, while it reproduced very well the C_5H_5 mole fraction profile. Very similar trends were reported by Saggese et al. [26], for C_5H_6, during their study on benzene pyrolysis and oxidation. On the other hand, our model gives a value for the phenyl radical (C_6H_5) maximum peak 5 times more important than the measured value. Similar results were reported by Tan and Frank [12] who mentioned that this finding is rather a good achievement since that most of the models published so far overpredict considerably the concentration of C_6H_5 of this flame; for example, Zhang and McKinnon's model [21] overpredicts phenyl by a factor of 8.

Concerning C_7 and C_8 species, our computation indicated that the proposed model gives a concentration of toluene 1.2 times less important than the experimental one, and a styrene mole fraction 1.1 times more important than the measured value. These predictions are very satisfactory as compared to the most recent benzene kinetic model proposed by Saggese et al. [26], where the computed toluene concentration was 2.2 times less important than the measured one, and the calculated styrene concentration was 3.7 times more important than the experimental value. On the other hand, our proposed model predicts a concentration of C_8H_2 150 times less important than the measured one. It is noteworthy that, at our knowledge, all the published models did not consider the C_8H_2 concentration calculations, thus we can't do any comparison.

In the case of polyaromatic hydrocarbons, our proposed model exhibits a very good capability in predicting $C_{10}H_8$, however underestimations were observed for indene (C_9H_8), for acenaphtene ($C_{12}H_8$) and for biphenyl ($C_{12}H_{10}$). Values of these underestimations were 1.7, 8 and 120 for C_9H_8, $C_{12}H_8$ and $C_{12}H_{10}$, respectively. These findings imply that much effort should be devoted to the enhancement of the $C_{12}H_{10}$ reproducibility.

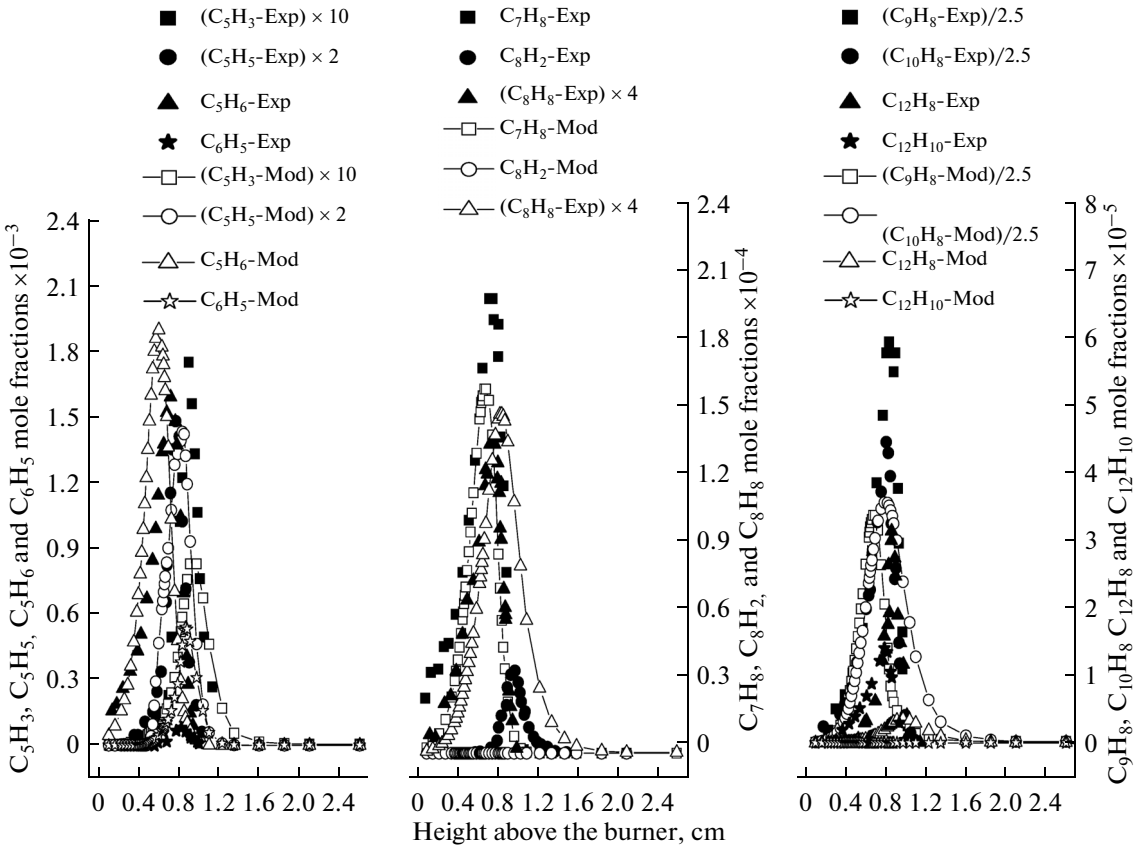

Fig. 3. Comparison between computed (lines + light symbols) and experimental ([6], dark symbols) C_5H_3, C_5H_5, C_5H_6, C_7H_8, C_8H_2, C_8H_2, C_8H_8, C_9H_8, $C_{10}H_8$, $C_{12}H_8$ and $C_{12}H_{10}$ mole fraction profiles.

Reaction Pathways

The pathway methodology has been previously reported [38]. In brief the appropriate subroutines in the Chemkin package (CKQYP, CKCONT), which systematically compute the rate of production and consumption of each species [40], were used to perform the pathway analysis. In these subroutines the involved reactions (for constants k) are sorted out with respect to their maximum absolute rate, and their sign indicated the species consumption or formation [43]. It is well known that the rate of progress is dependent on the species concentration and the temperature as well; these two entities are dependent on the location. So, in order to take this variation along the burner axis into account, integration of the rate of progress versus the height above the burner was chosen to consider the species molar flux. The integrated rate of progress for each reaction or group of reactions represents the contribution of this reaction or group of reactions to the species formation or consumption (according to the sign of the rate of progress). In the aim to describe the benzene oxidation pathways, rates of consumption and production were computed for every species. It is noteworthy that in this section, only the main reactions that have an important role in chemicals belonging to the studied system will be presented. The numbers in parentheses correspond to the numbers of reaction in the benzene mechanism.

The routes of benzene consumption are well documented [3, 25]. As the sp^2 C–H bond in benzene (112 kcal/mol) is weaker than the C–C bond in the ring (~136 kcal/mol), it is accepted that the initiation step in the thermal decomposition of benzene involves an ejection of a hydrogen atom by breaking one of the six C–H bonds in the molecule [44]. Thus, after the initial decomposition of benzene, the expected major paths consuming fuel is the H, O and OH attack leading to H abstraction, according to:

$$C_6H_5 + H = C_6H_6\text{ , (reverse reaction 663)}$$
$$C_6H_6 + H = C_6H_5 + H_2, \quad (654)$$
$$C_6H_6 + OH = C_6H_5 + H_2O, \quad (658)$$
$$C_6H_6 + O = C_6H_5O + H. \quad (657)$$

The flux analysis indicated that benzene conversion increased with increasing the height above the burner to reach a maximum at about 1.1 cm and remain constant afterward. On the other hand, the analysis of the net rates of benzene depletion showed that, closer to the burner which means at lower C_6H_6 conversions, hydrogen abstraction through reactions 654, 657 and 658 were found to be the most important

benzene consumption pathways, whereas the thermal decomposition of benzene via the reverse reaction 663 played a minor role. However, the contribution of this latter reaction increased upon raising the benzene conversion to reach a maximum in the reaction zone and then decreased (Fig. 4). It is noteworthy that, in the flame zone, the reaction (reverse 663) contributed with 73% in the benzene depletion, whereas reactions 654, 657 and 658 contributed with 15, 3.9 and 8.1%, respectively. These observations suggest that, for the studied flame, reaction of benzene with atomic oxygen to give phenoxy (reaction 657) did not contribute significantly to the C_6H_6 consumption. These findings are somewhat in disagreement with those reported by Tan and Frank [12] who mentioned that the reaction of benzene with hydroxyl atoms (reaction 658) was the most predominant benzene consumption channel, whereas the reaction with hydrogen atoms (reaction 654) was only of minor importance. The authors also reported that the decomposition reaction of benzene (reverse reaction 663) becomes important only at temperatures above 1400 K. In addition, the model proposed by Ristori et al. [22] confirmed that benzene oxidation was governed mainly by the reaction 657, whereas pathways leading to phenyl formation by H abstraction reactions of C_6H_6 with the H atom (reaction 654) and with the OH radical (reaction 658) were found to be of less importance. On the other hand and in agreement with our results, Richter and Howard [3] demonstrated, by using pathway analysis, that benzene was mostly transformed into the phenyl radical by reactions 654 and 658. Similar trends were also reported by Vourliotakis et al. [25] and by Saggese et al. [26] who mentioned that the most favored decomposition path of benzene was phenyl radical formation through reactions with H and OH radicals. Reaction 654 was the dominant phenyl formation path in rich flames conditions, while reaction 658 dominated under stoichiometric and lean environments.

When formed phenyl reacts mainly with hydrogen radicals and oxygen molecules to give benzyne (cyclo-C_6H_4), phenoxy–(C_6H_5O) and benzoquinones (o-$C_6H_4O_2$ and p-$C_6H_4O_2$). Benzyne undergoes a linearization to yield 3-hexene-1,5-diyne (l-C_6H_4), whereas phenoxy radical reacts with HO_2 to give phenol which undergoes an abstraction reaction with hydrogen atoms to give back phenoxy. On the other hand, o-benzoquinone decomposes to give cyclopentadienone (C_5H_4O) and CO, whereas p-benzoquinone may undergo a monomolecular decomposition yielding cyclopentadienone, or react with hydrogen atoms to give cyclopentadienoxy radicals (C_5H_5O) and CO. In addition, once formed, 3-hexene-1,5-diyne reacts with hydrogen radicals to give acetylene and n-C_4H_3 radicals, whereas cyclopentadienone may decompose to yield acetylene and carbon monoxide, or react with hydrogen atoms to give 1,3-butadienyl (1,3-C_4H_5). Furthermore cyclopentadienoxy radicals undergo monomolecular decomposition to give 1,3-butadienyl

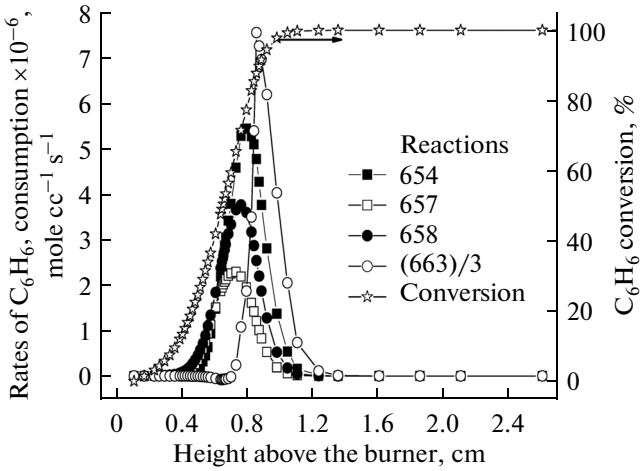

Fig. 4. Variation of the benzene conversion and the C_6H_6 consumption rates with the height above the burner.

and carbon monoxide (see Scheme). On the other hand, 1,3-C_4H_5 may decompose to give acetylene and vinyl radical (C_2H_3) or isomerize to give 1,2-butadienyl (1,2-C_4H_5) which may react with H or OH radicals to give vinylacetylene (C_4H_4) or with O atoms to yield ketene (CH_2CO) and vinyl radical. At its turn, vinylacetylene exhibits two depletion channels, the first leading to n-C_4H_3 via abstraction reactions with H or OH and the second leading to cyclopentadiene (cyclo-C_5H_6) via the recombination with methylene triplet (CH_2(T)). n-C_4H_3 can isomerize to i-C_4H_3 or react with hydrogen atoms to produce diacetylene (C_4H_2), which reacts mainly with hydrogen radicals to give butadiynyl (C_4H). This latter species (C_4H) reacts with oxygen molecules to produce ethynyl radical (C_2H) and carbon monoxide. Besides, the pathway analysis results indicate that two main routes contribute to the ethynyl radical consumption; the first is its reaction with acetylene giving diacetylene and hydrogen atoms, whereas the second is reactions with hydrogen and water molecules yielding acetylene. A minor path leads to carbon monoxide and hydrogen atoms.

Concerning acetylene, which is thought to be one of the main PAH building blocks through the HACA mechanism [5, 45–47], flux analysis showed that C_2H_2 depletion was mainly governed by the set of reaction:

$$C_2H_2 + O = HCCO + H, \quad (146)$$

$$C_2H_2 + C_2H = C_4H_2 + H, \quad (476)$$

$$CH + C_2H_2 = \text{cyclo-}C_3H_2 + H, \quad (44)$$

$$C_2H_2 + OH = CH_2CO + H, \quad (148)$$

$$C_2H_2 + O = CH_2(T) + CO. \quad (145)$$

It was found that 53% of acetylene was consumed via its oxidation by oxygen atoms leading to ketone radical (146), whereas only 6% of acetylene consumption was realized by the reaction (145).

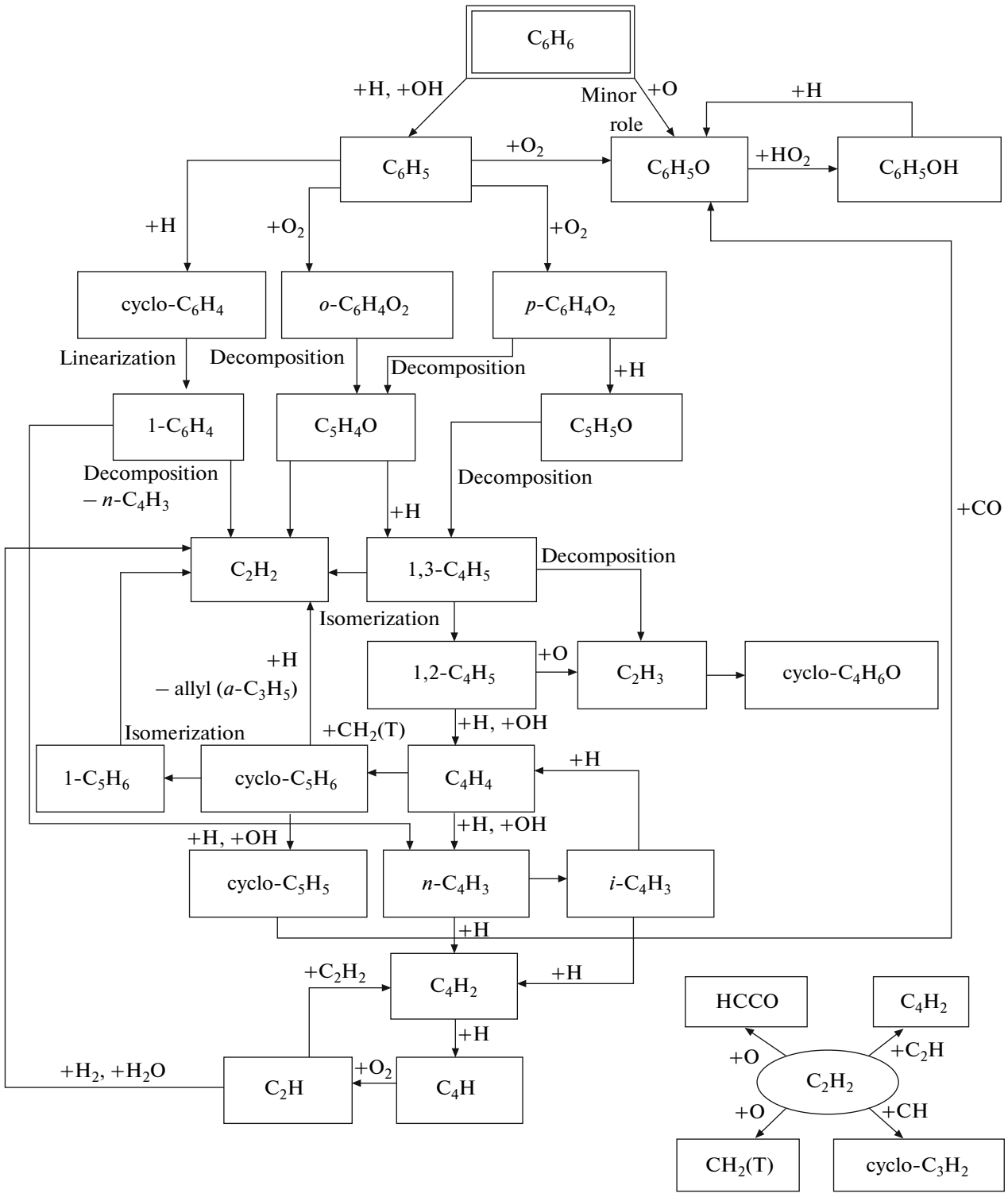

Concerning C_5 species, our computations indicated that cyclopentadiene may react with hydrogen radical to produce acetylene, allyl–C_3H_5 and cyclopentadienyl radicals, or isomerize to give linear C_5H_6, or undergo a monomolecular decomposition yielding acetylene or finally react with hydroxyl radicals to produce C_5H_5. On the other hand, cyclopentadienyl (C_5H_5), which is considered as one of the most important intermediate in PAH formation due to its neutrality and ambident-reactivity at different sites [48], reacts mainly with carbon monoxide to produce phenoxy (Scheme).

Compare with the experimental work of Bittner and Howard, benzene combustion was investigated

numerically (using kinetic modeling). The data collected reveal the following.

1. The computed mole fraction profiles of reactants (benzene and oxygen) as well as those of the major stable species were in good agreement with those measured experimentally.

2. The proposed model was able to predict, with a reasonably level of accuracy, mole fraction profiles of methyl radical, methane, acetylene, propargyl and cyclopentadienyl radicals.

3. The proposed model exhibited a very good capability in predicting toluene (C_7H_8) and styrene (C_8H_8), whereas it fails to predict the concentration of C_8H_2 (the computed value was 150 times less important than the measured one).

4. A good reproducibility was observed for $C_{10}H_8$, however underestimations were observed for C_9H_8, $C_{12}H_8$, and $C_{12}H_{10}$. These findings imply that some work must be done for enhancing the reproducibility of these species especially for $C_{12}H_{10}$.

5. Benzene depletion was dependent on its conversion. Hydrogen abstraction reactions governed the benzene consumption at lower conversions, whereas the C_6H_6 thermal decomposition was found to be the most important depletion path at medium and higher conversions. On the other hand, whatever the conversion, reaction of benzene with atomic oxygen to give phenoxy was found to play a minor role in C_6H_6 consumption. It is noteworthy that these findings are almost new, because to our knowledge, the dependence of benzene depletion pathway on the C_6H_6 conversion was not proposed in any of the published models.

REFERENCES

1. Sivaramakrishnan, R., Brezinsky, K., Vasudevan, H., and Tranter, R.S., *Combust. Sci. Technol.*, 2006, vol. 178, p. 285.
2. Xu, C., Braun-Unkhoff, M., Naumann, C., and Frank, P., *Proc. Combust. Inst.*, 2007, vol. 31, p. 231.
3. Richter, H. and Howard, J.B., *Phys. Chem. Chem. Phys.*, 2002, vol. 4, p. 2038.
4. Defoeux, F., Dias, V., Renard, C., Van Tigglen, P.J., and Vandooren, J., *Proc. Combust. Inst.*, 2005, vol. 30, p. 1407.
5. Detilleux, V. and Vandooren, J., *Combust., Explos. Shock Waves*, 2009, vol. 45, p. 392.
6. Bittner, J.D. and Howard, J.B., *Proc. Combust. Inst.*, 1981, vol. 18, p. 1105.
7. Alzueta, M.U., Glarborg, P., and Dam-Johansen, K., *Int. J. Chem. Kinet.*, 2000, vol. 32, p. 498.
8. Chai, Y. and Pfefferle, L.D., *Fuel*, 1998, vol. 77, p. 313.
9. *Soot Formation in Combustion*, Bockhorn, H., Ed., Berlin: Springer, 1994.
10. Chiang, H.-M., *PhD Dissertation*, Newark, N.J.: Inst. of Technology, 1995.
11. Brukh, R., Salem, T., Slanvetpan, T., Barat, R., and Mitra, S., *Adv. Environ. Res.*, 2002, vol. 6, p. 359.
12. Tan, Y. and Frank, P., *Proc. Combust. Inst.*, 1996, vol. 26, p. 677.
13. Richter, H., Benish, T.G., Mazyar, O.A., Green, W.H., and Howard, J.B., *Proc. Combust. Inst.*, 2000, vol. 28, p. 2609.
14. Dupont, L., El Bakali, A., Pauwels, J.-F., DaCosta, I., Meunier, P., and Richter, H., *Combust. Flame*, 2003, vol. 135, p. 171.
15. Shandross, R.A., Longwell, J.P., and Howard, J.B., *Proc. Combust. Inst.*, 1996, vol. 26, p. 711.
16. Tregrossi, A., Ciajolo, A., and Barbella, R., *Combust. Flame*, 1999, vol. 117, p. 553.
17. Mackinnon, J.T. and Howard, J.B., *Proc. Combust. Inst.*, 1992, vol. 24, p. 965.
18. Grieco, W.J., Lafleur, A.L., Swallow, K.C., Richter, H., Taghizadeh, K., and Howard, J.B., *Proc. Combust. Inst.*, 1998, vol. 27, p. 1669.
19. Yang, B., Li, Y., Wei, L., Huang, C., Wang, J., Tian, Z., Yang, R., Sheng, L., Zhang, Y., and Qi, F., *Proc. Combust. Inst.*, 2007, vol. 31, p. 555.
20. Lindstedt, R.P. and Skevis, G., *Combust. Flame*, 1994, vol. 99, p. 551.
21. Zhang, H.Y. and McKinnon, J.T., *Combust. Sci. Technol.*, 1995, vol. 107, p. 261.
22. Ristori, A., Dagaut, P., Pengloan, G., and Cathonnet, M., *Combust. Sci. Technol.*, 2001, vol. 167, p. 223.
23. D'Anna, A. and Violi, A., *Proc. Combust. Inst.*, 1998, vol. 27, p. 425.
24. Richter, H., Grieco, W.J., and Howard, J.B., *Combust. Flame*, 1999, vol. 119, p. 1.
25. Vourliotakis, G., Skevis, G., and Founti, M.A., *Energy Fuels,* 2011, vol. 25, p. 1950.
26. Saggese, C., Frassoldati, A., Cuoci, A., Faravelli, T., and Ranzi, E., *Combust. Flame*, 2013, vol. 160, p. 1168.
27. Burcat, A., Snyder, C., and Brabbs, T., *Ignition Delay Times of Benzene and Toluene with Oxygen in Argon Mixtures*, NASA TM-87312, 1986.
28. Emdee, J.L., Brezinsky, K., and Glassman, I., *J. Phys. Chem.*, 1992, vol. 96, p. 2151.
29. Lovell, A.B., Brezinsky, K., and Glassman, I., *Int. J. Chem. Kinet.*, 1989, vol. 21, p. 547.
30. Alzueta, M.U., Oliva, M., and Glarborg, P., *Int. J. Chem. Kinet.*, 1998, vol. 30, p. 683.
31. Detilleux, V. and Vandooren, J., *J. Phys. Chem. A*, 2009, vol. 113, p. 10913.
32. Tsang, W. and Hampson, R.F., *J. Phys. Chem. Ref. Data*, 1986, vol. 15, p. 1087.
33. Bohland, T., Dobe, S., Temps, F., and Wagner, H.G., *Ber. Bunsen-Ges. Phys. Chem.*, 1985, vol. 89, p. 432.
34. Bergeat, A., Calvo, T., Caralp, F., Fillion, J.H., Dorthe, G., and Loison, J-C., *Faraday Discuss.*, 2001, vol. 119, p. 67.
35. Hidaka, Y., Shiba, S., Takuma, H., and Suga, M., *Int. J. Chem. Kinet.*, 1985, vol. 17, p. 441.

36. Hidaka, Y., Higashihara, T., Ninomiya, N., Oki, T., and Kawano, H., *Int. J. Chem. Kinet.*, 1995, vol. 27, p. 331.

37. Dagaut, P. and Kurylo, M.J., *J. Photochem. Photobiol., A*, 1990, vol. 51, p. 133.

38. Hamdane, S., Rezgui, Y., and Guemini, M., *Kinet. Catal.*, 2012, vol. 53, p. 648.

39. Tsang, W., *J. Phys. Chem. Ref. Data*, 1987, vol. 16, p. 471.

40. Kee, R.J., Grcar, J.F., Smooke, M.D., and Miller, J.A., *A FORTRAN Program for Modeling Steady Laminar One Dimensional Premixed Flames*, Report SAND85-8240, Livermore: Calif.: Sandia National Laboratories, 1985..

41. D'Anna, A. and Violi, A., *Energy Fuels*, 2005, vol. 19, p. 79.

42. Djurisic, Z.M., Joshi, A.V., and Wang, H., *Second Joint Meeting of the U.S. Sections of the Combustion Institute*, Oakland, Calif., 2001, p. 8.

43. Lamoureux, N., El-Bakali, A., Gasnot, L., Pauwels, J.F., and Desgroux, P., *Combust. Flame*, 2008, vol. 153, p. 186.

44. Laskin, A. and Lifshitz, A., *Proc. Combust. Inst.*, 1996, vol. 26, p. 669.

45. Wang, D., Violi, A., Kim, D.H., and Mullholland, J.A., *J. Phys. Chem. A*, 2006, vol. 110, p. 4719.

46. Wang, H. and Frenklach, M., *Combust. Flame*, 1997, vol. 110, p. 173.

47. Frenklach, M. and Warnatz, J., *Combust. Sci. Technol.*, 1987, vol. 51, p. 265.

48. McEnally, C.S. and Pfefferle, L.D., *Combust. Sci. Technol.*, 1998, vol. 131, p. 323.